(IJRST) 2016, Vol. No. 6, Issue No. IV, Oct-Dec e-ISSN: 2249-0604, p-ISSN: 2454-180X

FINITE ELEMENT ANALYSIS OF MAGNETIC FIELD EFFECT ON CRYOCOOLER REGENERATORS

Rajendra Kumar[1] and Sumit Shoor[2]
School of Mechanical Engineering
Lovely Professional University
Phagwara, Punjab, India

ABSTRACT

Regenerative type of cryocoolers employ magnetic intermetallic compounds of 3d transition and 4f heavy rare earth elements in the regenerators to work well below 10 K. Cryocoolers are used extensively in MRI and SQUIDS to achieve temperatures of ~4 K. Therefore they are always inevitably exposed to high magnetic fields ~5 T-7 T and their performance is degraded. Except for magnetic noises, induction losses are also present in regenerators. This paper discusses the Joule heat generation in regenerators of cryocoolers under magnetic fields of 1 T, 3 T and 4.3 T. Commercial code of FEA package, ANSYS-APDL 14.5 is used to evaluate the heat generated at above stated magnetic fields. The values obtained from FEA for heat generation is highest at 4.3 T.

Keywords: *Cryocoolers; Finite Element Analysis (FEA); Joule heating; ANSYS; Magnetic field distribution*

1. INTRODUCTION

Cooling devices/systems capable of producing temperature below 120 K are known as cryogenic refrigerators or simply, cryocoolers[1]. These are of two types namely, recuperative and regenerative cryocoolers[2]. Regenerative cryocoolers are again of mainly three types, Stirling, Gifford- McMahon (GM) and pulse tube cryocoolers (PTC).

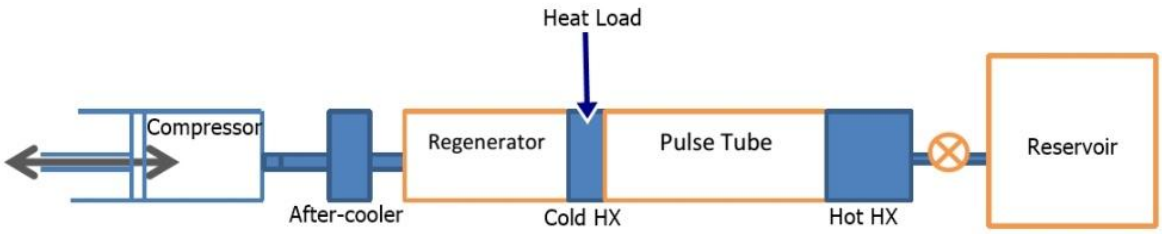

Figure 1: Pulse Tube Cryocooler (Orifice PTC)

The performance of such a system is directly dependent upon its regenerator effectiveness. The conventional cryogenic regenerator materials are stainless steel or bronze woven mesh screens and lead spherical balls for temperature ranges 30 K-300 K and 10 K-30 K respectively. However, below 10 K heat capacity of lead decreases drastically and magnetic intermetallic compounds[3], [4] are used in regenerators to achieve temperatures of 4 K due to their increased specific heat below 10 K. Due to this advancement the

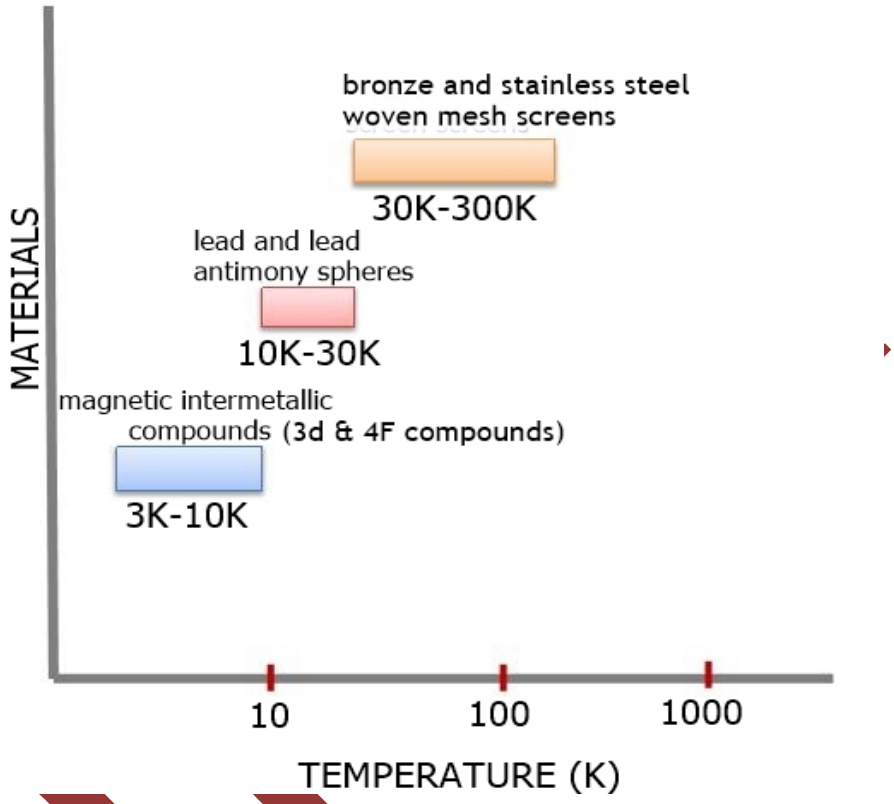

Figure 2: Temperature ranges for regenerator materials used in cryocoolers

use of low-temperature mechanical cryocooler has increased drastically. These are extensively used for cooling purpose in MRI and magnetometers (e.g. SQUID). Therefore they are inevitably exposed to high magnetic fields ranging from 1 T to 7 T or even more. This causes the occurrence of magnetic noises in the regenerator containing magnetic materials[5]–[7] in turn, the performance of cryocooler is affected. So far, the electrical resistivity of regenerator material is not considered for the possible induction losses that could occur under the influence of magnetic fields.

This paper presents the evaluation of Joule heating for cryocooler regenerator materials using a commercial code of ANSYS APDL 14.5 package, while cold end temperature is varied from 4.2 K to 10 K. The problems posed while selecting the regenerator material is discussed. The magnetic field distribution is matched with the heat generation. At last, the temperature profiles for various cold end temperatures are compared. The values obtained suggest that electrical properties should be considered for regenerator materials when desired cooling power ~mW.

2. REGENERATOR MATERIAL SELECTION

The magnetic intermetallic compounds are often selected on the basis of their specific heat, primarily for cryogenic regenerators. Therefore thermal, electrical and magnetic properties are not specified simultaneously for such materials. The data present in the literature about the magnetic properties and electrical properties are very limited when it comes to regenerator materials. Therefore, the material selected for numerical analysis in the present work is one whose relative permeability is present in the literature. Relative permeability(μ_r) is affected by non-linear behavior of magnetic materials greatly.

As seen from reference 3 the first most material used below 10 K wasEr_3Ni. Its specific heat values are different in various works. Hershberg et al[8] have reported the test results of volumetric and mass heat capacity ofEr_3Ni fabricated sample. The anomalies in the peak values of different sample were seen and the reason for it was attributed to the different methods adopted to fabricate same material by different researchers.

The magnetic properties of this material is reported by Tristan et al[9]. However, no interpretation can be made for non-linear behavior of relative permeability ofEr_3Ni. Talik[10] has reported the magnetization ofEr_3Ni. Since these works are relevant from the point of view of relative permeability, the results reported by Paccard, Becle and Lemaire[11] and interpreted by Fujimoto et al[5] is used. The non-linear behavior is encountered by considering the influence of magnetic field on the heat capacity and is explained below along with the magnetic properties of it.

A) Magnetic properties of Er_3Ni

The magnetic properties present in literature are already discussed in chapter 2. The relative permeability of Er_3Ni (linear and constant) is taken to be 1.3from reference 11 and 5. Magnetic materials require either relative permeability or B-H curve as input in ANSYS. However, if both are given then relative permeability is used for calculations rather than aB-H curve.

B) Electrical resistivity ofEr_3Ni

When the magnetic materials are subjected to varying magnetic field then induction heating of the matrix material is also likely to take place. This would lead to induced current density in the regenerator and temperature profile will be shifted to the higher side depending upon the magnetic flux density incident upon the regenerator. It is a temperature dependent property. The electrical resistivity (ρ) of Er_3Ni is taken from the work of Talik[12].

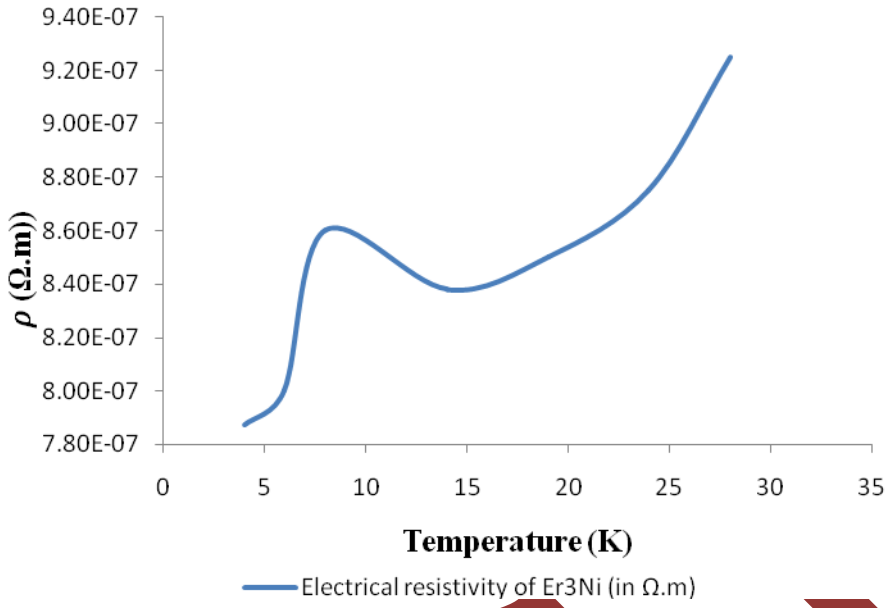

Figure 3: Electrical resistivity of Er_3Ni

C) Thermal properties of Er_3Ni

The thermal properties include thermal conductivity and specific heat of the material. The Nèèl temperature (T_N) and density for Er_3Ni are taken as **7.7 K**[13] **and 9290 kg/m^3** respectively.

Thermal conductivity is taken as **2 W/m K and 0.3 W/m K at 50 K and 5 K** respectively[14].

For regenerator materials, heat capacity is expressed volumetrically and its units are J/cm^3 K. Therefore it is necessary to convert it to J/ kg K to put it into ANSYS.

$$1\frac{J}{cm^3\ K}\times\frac{1}{Density\left(in\frac{g}{cm^3}\right)}=1\frac{J}{g\ K}\times\frac{1}{10^{-3}}=1\frac{J}{kg\ K}$$

Specific heat for the present analysis is considered to be a function of magnetic field and temperature as well. Therefore temperature and magnetic field dependent values are used in ANSYS. The work by Tokai et al[15] is the only work present till date to refer to the effect of magnetic field on the heat capacity of Er_3Ni and is shown in figure 4.

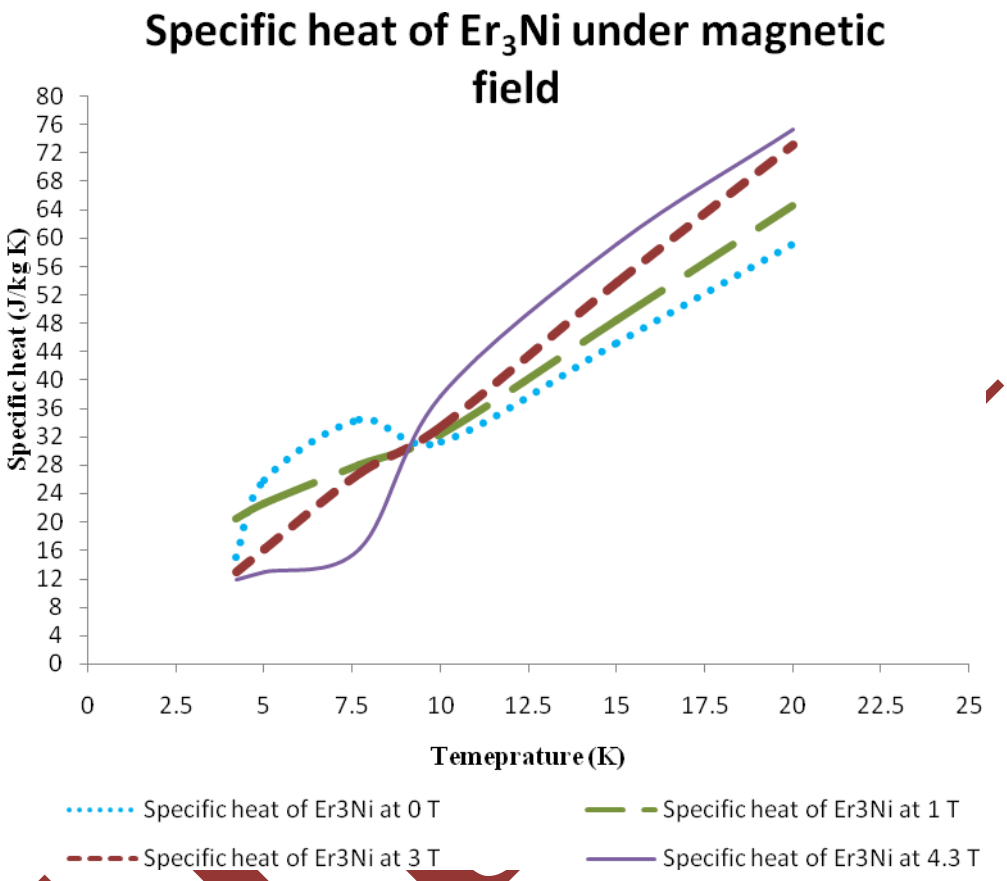

Figure 4: Specific heat of Er_3Ni under magnetic field

3. FINITE ELEMENT MODEL

The computational domain, meshing of the model, loads and boundary conditions used is discussed in the following parts of this section.

3.1 COMPUTATIONAL DOMAIN

The solid model consists of the regenerator and a solenoid/coil. The presence of solenoid produces non-uniform magnetic field and hence the model becomes more practical. A 2D axisymmetric model is considered for the analysis. The coil is symmetrical with the regenerator. However, while doing so the regenerator becomes small in comparison to the coil. The regenerator length is taken to be 100 mm and its width is 20 mm. The magnetic field is restricted to the domain while making a boundary around the coil and regenerator. Figure 5 shows the problem domain of the model.

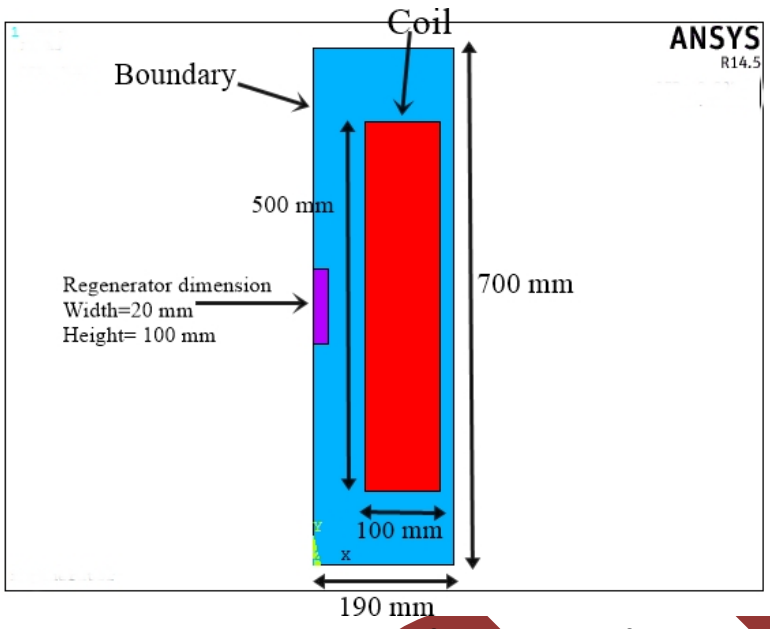

Figure 5: Regenerator under non-uniform magnetic field (with coil)

3.2 MESHING OF MODEL

Plane 13 (vector quad 13), a coupled field quadrilateral element is used in the analysis. It allows for 2D thermal, magnetic, and electrical field calculations with limited coupling between the fields. PLANE13 is defined by four nodes with up to four degrees of freedom per node. The element has the nonlinear magnetic capability for modeling B-H curves of the material considered. It can be meshed in quadrilateral as well in triangular forms.

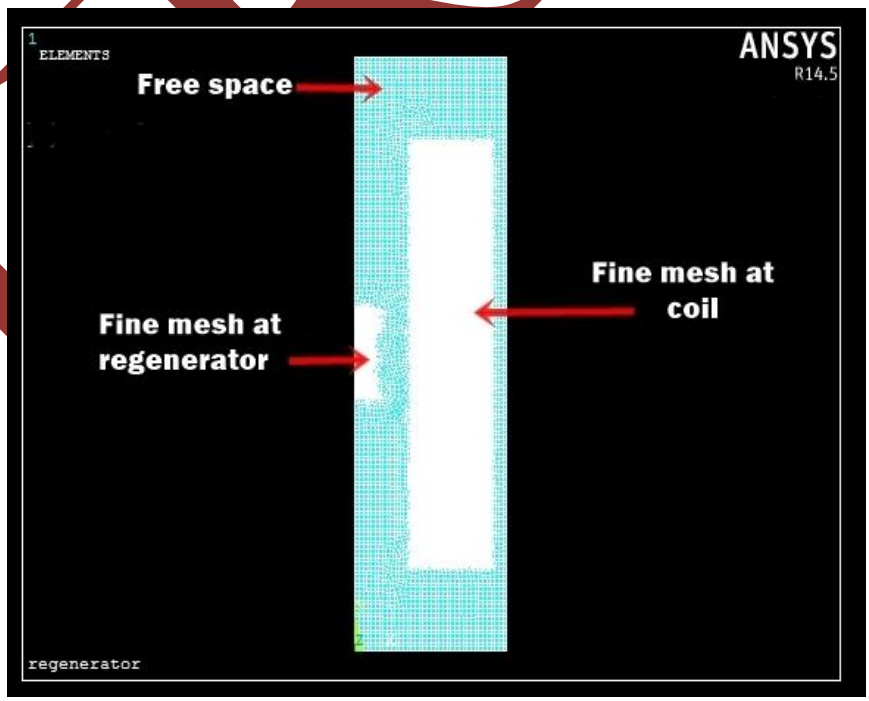

Figure 6: Meshed model

Since the regenerator area is of interest, therefore fine meshing can be seen at it. This leads to faster convergence rate and less computational time. The validation of mesh size is done by continuously refining the initial guess. At last a mesh size of 0.0005 is found to be optimal.

3.3 LOADS

For a coupled field analysis two types of loads are applied to the model namely, thermal and magnetic loads. Since the heat capacities are obtained at 1 T, 3 T and 4.3 T magnetic fields, therefore current density (J) on the coil is applied to obtain these values of magnetic flux incident upon the regenerator.

Table 1: Magnetic loads- values of current density (J) corresponding to magnetic flux density (B)

Sr. No.	Magnetic flux density, B	Current density, J
1	1 T	$1.08793 \times 10^7 A/m^2$
2	3 T	$3.2638 \times 10^7 A/m^2$
3	4.3 T	$4.67812 \times 10^7 A/m^2$

The thermal load here is the heat generated from magnetic analysis and is put back to the thermal analysis.

3.4 BOUNDARY CONDITIONS

The boundary conditions for the model is a magnetic flux density of 1 T, 3 T and 4.3 T. The temperature of the hot end, i.e. upper end of the regenerator is fixed at 20 K and the cold end temperature, i.e. the lower end of regenerator is taken as 4.2 K, 6 K, 8 K and 10 K. The magnetic field is made non-uniform by taking the vector potential in the z-direction (circumferential direction) as zero at the boundary lines shown in figure 5.

$$\frac{\partial A_z}{\partial \phi} = 0 \qquad (1)$$

4. GOVERNING EQUATIONS

The electromagnetic part of induction heating is controlled by Maxwell's equations, as follows:

$$\nabla . \boldsymbol{D} = \rho_f \qquad (2)$$

$$\nabla . \boldsymbol{B} = 0 \qquad (3)$$

$$\nabla \times \boldsymbol{E} = -\frac{\partial \boldsymbol{B}}{\partial t} \qquad (4)$$

$$\nabla \times \boldsymbol{H} = \boldsymbol{J}_f + \frac{\partial \boldsymbol{D}}{\partial t} \qquad (5)$$

Where ***D*** is the electric flux density, ***B*** is the magnetic flux density, ***E*** is the electric field, ***H*** is the magnetic field, $\boldsymbol{J}_f$ is the free currentdensity, $\rho_f$is the free charge density, *t* is the time. Relating ***D*** and ***H*** in terms of ***E*** and ***B*** depends on the material, and for linear mediait can be related through the following constitutive relations:

$$\boldsymbol{D} = \varepsilon_0 \varepsilon_r \boldsymbol{E} \quad (6)$$

$$\boldsymbol{B} = \mu_0 \mu_r \boldsymbol{H} \quad (7)$$

Where, $\varepsilon_0 = 8.854 \times 10^{-12}\ F/m$ is the vacuum permittivity.

$\mu_0 = 4\pi \times 10^{-7}\ H/m$ is the permeability.

$\varepsilon_r$and $\mu_r$are relative permittivity and permeability respectively. Current density and electric field are related by Ohm's law:

$$\boldsymbol{J} = \sigma . \boldsymbol{E} \quad (8)$$

Where, σ is the electrical conductivity.

Combining Maxwell's eq. 2-5 and constitutive Eqn. 6-8 leads to the following complex diffusion eqn.:

$$\frac{1}{\mu}\nabla^2 \bar{\boldsymbol{A}} + \iota\omega\sigma\bar{\boldsymbol{A}} = -\boldsymbol{J_s} \quad (9)$$

For the case of induction heating it is the time average Joule heat density that comes from the induced Eddy currents which is of interest and can be derived from eqn. 9 as:

$$\boldsymbol{J_e} = -\iota\omega\sigma\bar{\boldsymbol{A}} \quad (10)$$

The joule heating is found using Joules law:

$$Q = \frac{1}{2\sigma}|J_e|^2 \quad (11)$$

5. RESULTS AND DISCUSSIONS

Thedegree of freedom (DOF) is magnetic flux density (BSUM) and Joule heat generation (JHEA). Now as the solenoid is on the right side of the regenerator, the magnetic field lines originate at right and move leftwards.

A) Magnetic flux distribution- Figure 7 shows the distribution of magnetic flux in the problem domain as well as on the regenerator.

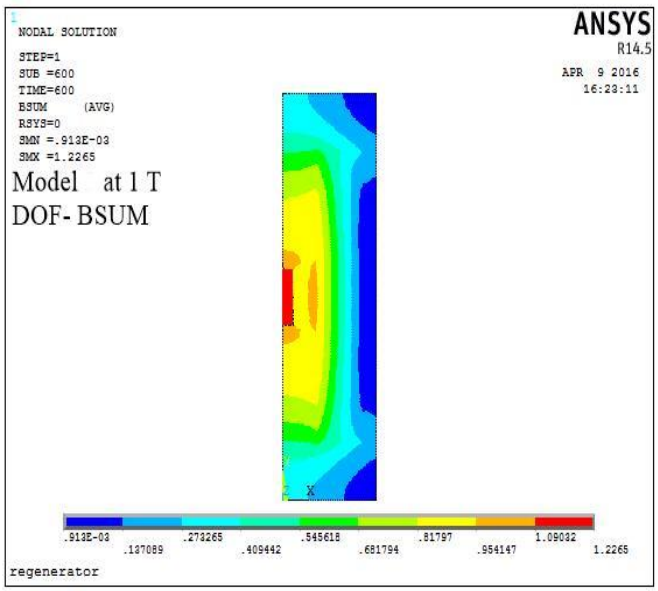

Figure 7a: Magnetic flux density at 1T FE domain

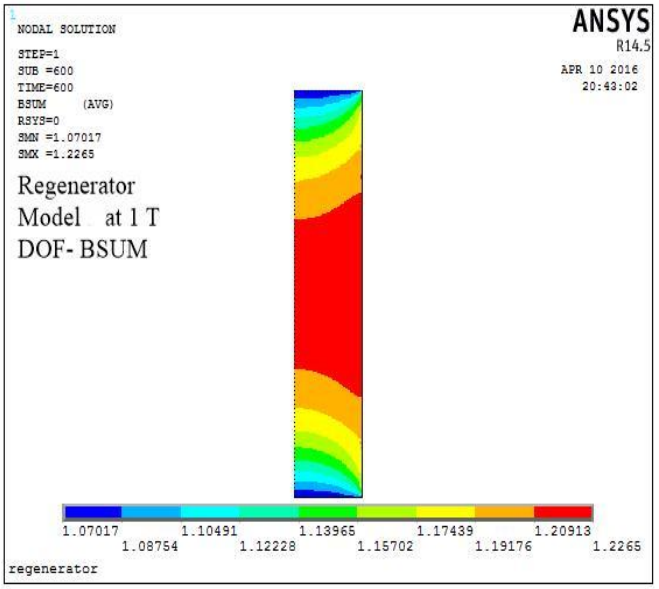

Figure 7b: Magnetic flux density at 1T on regenerator

The magnetic flux distribution is necessary to be evaluated at different points in the regenerator, to see the effect of heating. In figure 7a it is seen that the maximum B is 1.22 T. The value exceeds 1 T due to the decimal points considered in the value of current density. The calculations in ANSYS is precise and hence values upto four places of the decimal are given in output. This is why the value of B on regenerator (figure 7b) varies from 1.07 T to 1.23 T rather than exactly be 1 T. The pattern of distribution of B is same as that of H, as evident from Eqn. 7. Similarly, the following figure 8 and 9 depict the distribution at 3 T and 4.3 T,

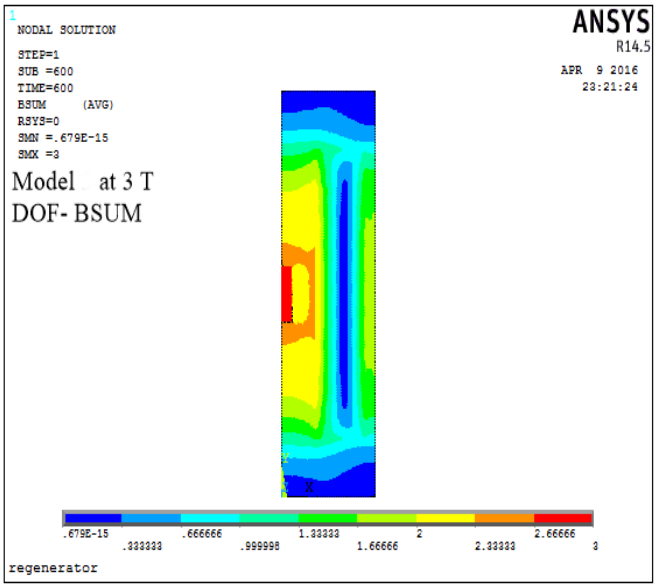

Figure 8a: Magnetic flux density at 3T FE domain

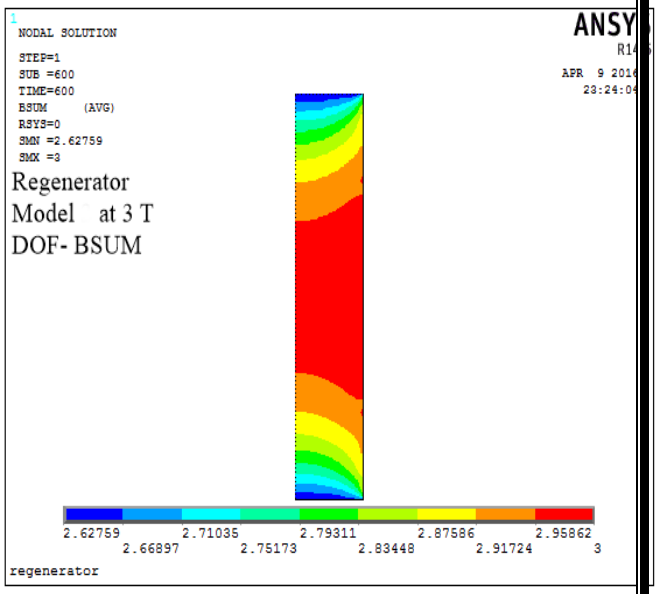

Figure 8b: Magnetic flux density at 3T on regenerator

From figure 8, the increase in the value of B from 1 T to 3 T has caused an increase in the flux density on the regenerator and area near it. It is very clearly seen that the flux distribution follows the same pattern as that of above case. Figure 9 shows the case of 4.3 T.

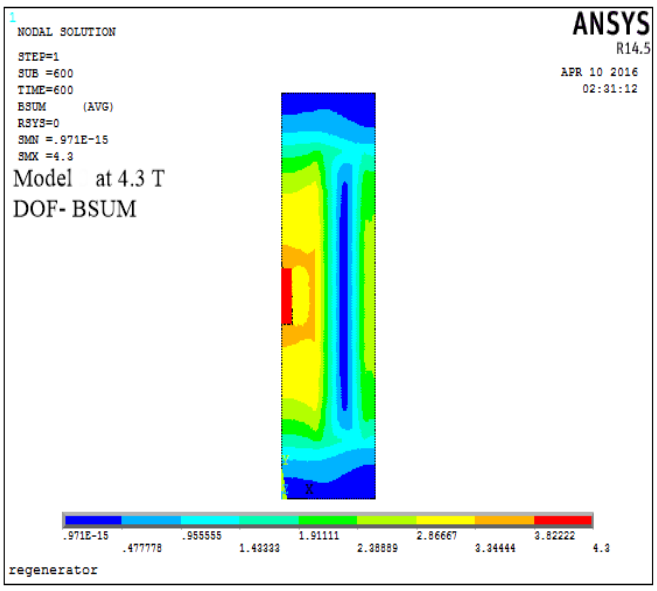

Figure 9a: Magnetic flux density at 4.3 T FE domain

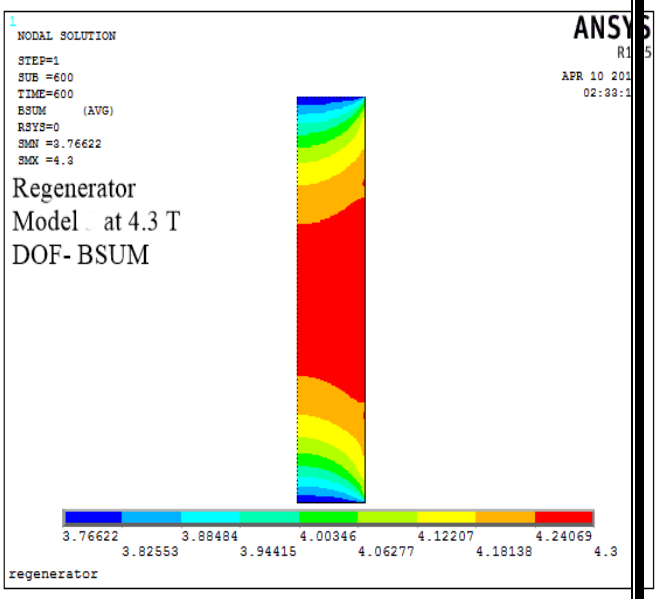

Figure 9b: Magnetic flux density at 4.3 T on regenerator

The distribution of magnetic flux density is important to note and it is matched with the Joule heat generation in the regenerator and the different areas for less or more heat generation can be identified

based on this model. Therefore, the following results show the heat generation in the regenerators at 1 T, 3 T and 4.3 T for the model.

B) Joule heat generation distribution- The following results show how much heat is generated when the electrical resistivity of the matrix material is considered and put into the material properties in ANSYS. The heat generation depends on upon the quantity of the matrix material used in regenerator since the heat generation is volumetric in nature. Also, the thermal conductivity causes the increase in axial and longitudinal heating of the regenerator bed.

Figure 10a, 10b and 10c show the results from a simulation of the heat generation for the model.

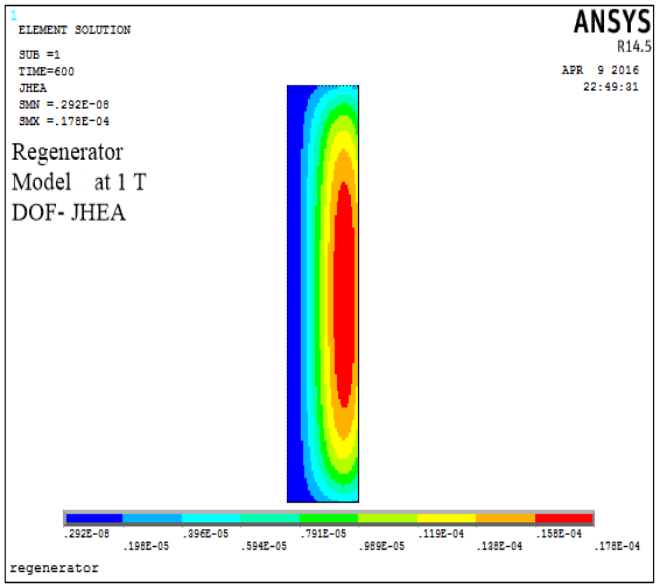

Figure 10a: Joule heat generation at 1T- regenerator for model 3

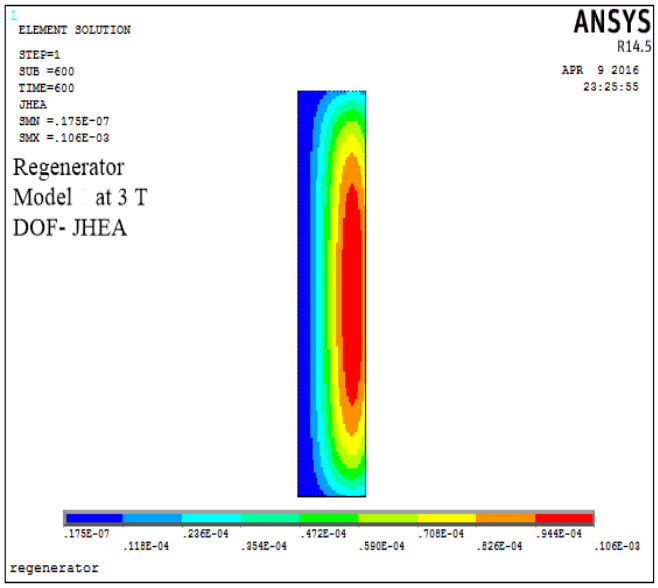

Figure 10b: Joule heat generation at 3T- regenerator for model 3

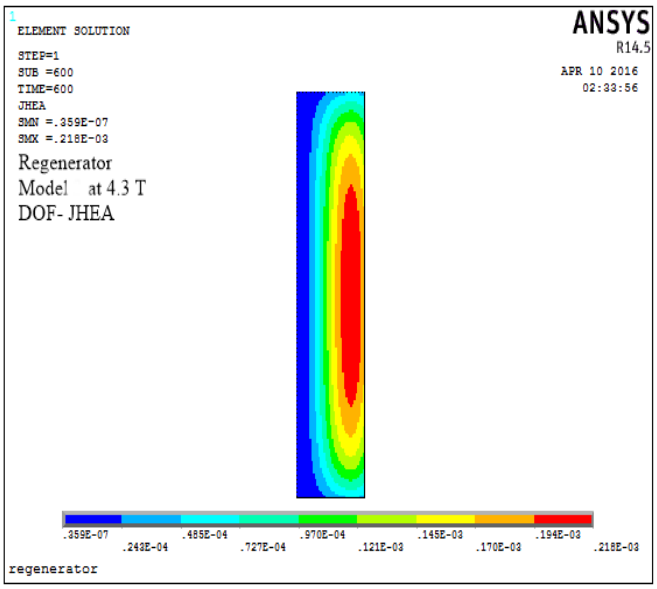

Figure 10c: Joule heat generation at 4.3T- regenerator for model 3

The resistivity of the material plays a crucial role in deciding the heat generation in the matrix material over the period of time. Cryocoolers, in particular, PTC, are manufactured so that they can run for 40000 hours or more and the time between maintenance is very large. However, the heat generation can hinder the regenerator over such a long period of time and these kinds of losses are material dependent.

The heat generated at 1 T for model 3 is of the order of μJ and is shown in figure 10a. The regions of maximum heat generation lie on the right side of regenerator. The reason to this is attributed to the penetration of magnetic flux lines inside the regenerator and the time period for which analysis has been done. When it is compared with heat generation at 3 T, then no appreciable change in distribution is observed. As far as the values are concerned, they are higher and the values are still in μJ.

In figure 10c it can be seen that the regions of heat generation are expanded and has also increased at the left side of regenerator near both the ends.

From these simulations, it can be seen that the maximum value of heat generation for 1 T, 3 T and 4.3 T is of the order of 0.178E-4 J, 0.106E-3 J and 0.218E-3 J respectively.

C) Temperature profile at different magnetic fields and cold end temperature- Now when the heat generated is put as the load in the thermal analysis[16] the change in the temperature profile is observed as the magnetic field increases and is shown as below.

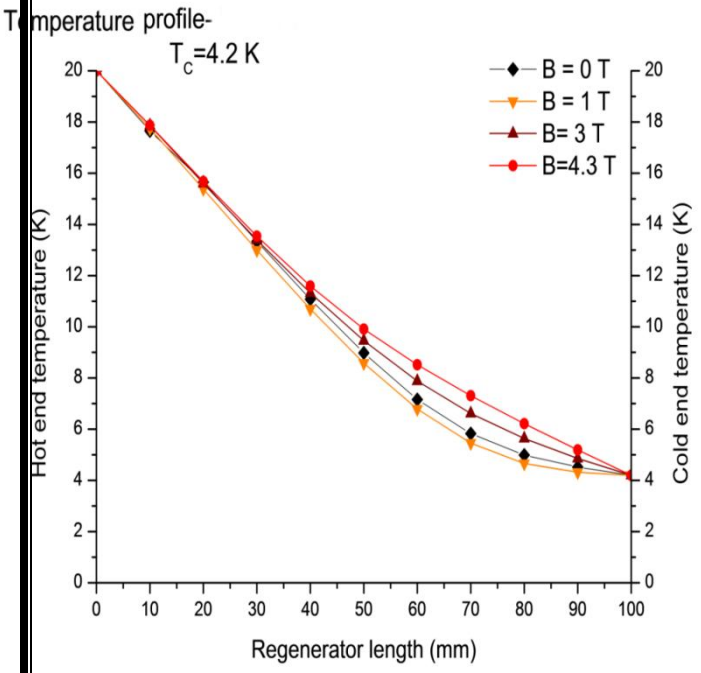

Figure 11: Temperature profile at $T_C = 4.2\ K$

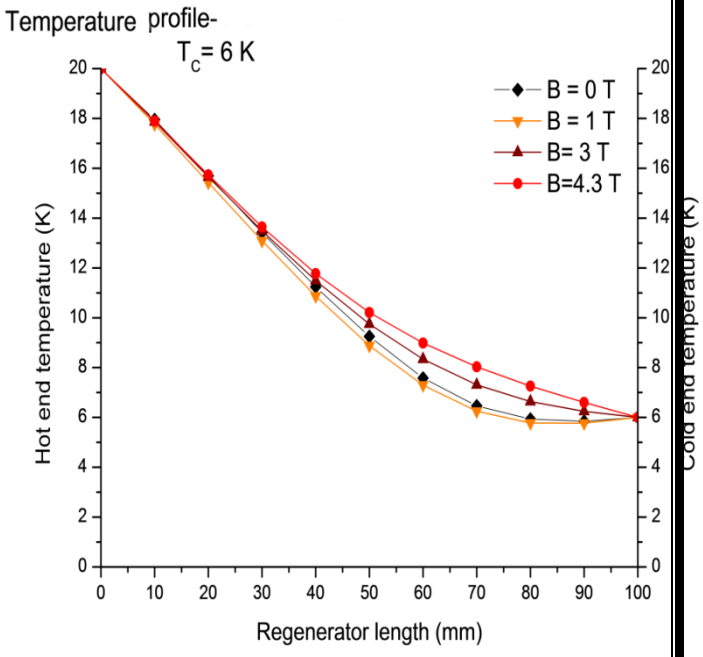

Figure 12: Temperature profile at $T_C = 6\ K$

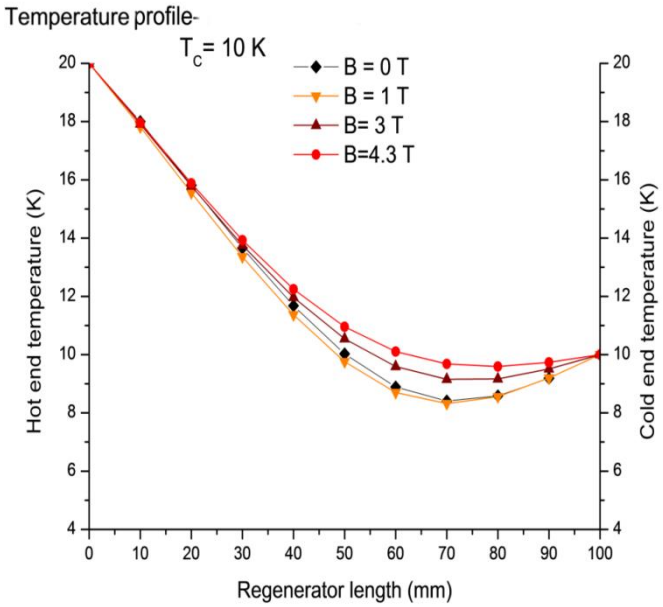

Figure 13: Temperature profile at $T_C = 8\,K$

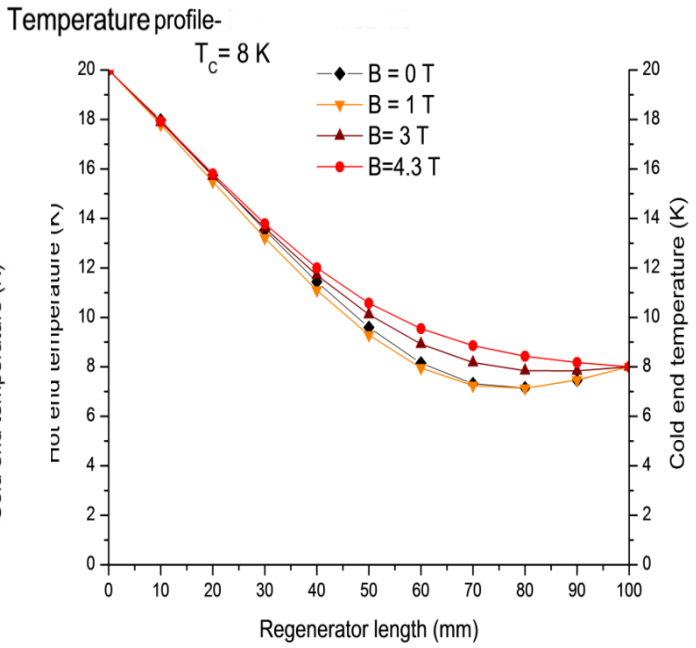

Figure 14: Temperature profile at $T_C = 10\,K$

With the increase in the cold end temperature, T_c the temperature profile begins shifting towards higher side in between 60 mm to 65 mm.The temperature along the length of regenerator for 1 T is less than 0 T. This is evident on the basis of the heat capacity of Er_3Ni at 1 T (refer figure 4). While the temperature at 3 T and 4.3 T are on higher side. This is due to the increased heat generation at elevated magnetic fields. The ineffectiveness of regenerators (figure 13 and 14) becomes greater at temperatures above 8 K and magnetic field of 4.3 T.

Therefore applying a magnetic flux density of 1 T gives rise to regions of lower temperatures as compared to 0 T, 3 T and 4.3 T. The uniformity in the temperature distribution results in the effective utilization of bed of regenerator when Er_3Ni is considered as matrix material.

6. CONCLUSIONS

In the present work, the electrical resistivity is considered for the cryocooler regenerator materials alongwith the magnetic and thermal properties, which is generally neglected. However due to the exposure to magnetic field, such cooling systems when operating at a temperature of 4 K are affected by the induction losses and Joule heating should be considered as a source of loss. Secondly, the dependence of specific heat on magnetic field for the regenerator materials must be considered. In addition to it, the magnetic behavior of the magnetic material is highly non-linear. Therefore, the relative permeability of the material must be found experimentally.Nowadays research to improve the thermal characteristics of liquid helium by adding nanoparticles is going on. However, the use of regenerative cryocoolers in places at high magnetic fields makes them more susceptible towards such

losses and magnetic noises, subjected to the magnetic behavior of nanoparticle added. The induction losses would be more prominent in magnetically augmented regenerators[16]–[18].

Therefore, it is concluded at the end that Joule heating should also be considered as the source of loss when cryocoolers are exposed to high magnetic fields subjected to the behavior of the matrix material. In case of Er_3Ni the ineffectiveness of the regenerator is observed at 3 T and 4.3 T from finite element analysis. Furthermore, the effectiveness of regenerator is a strong function of the heat capacity of the regenerator materials.

REFERENCES

[1] G. Walker, *Cryocoolers*, 1st ed, Springer US 1983.

[2] R. Radebaugh, "Cryocoolers: the state of the art and recent developments.," *J. Phys. Condens. Matter*, vol. 21, no. 16, p. 164219, 2009.

[3] T. Kuriyama, R. Hakamada, H. Nakagome, Y. Tokai, M. Sahashi, R. Li, O. Yoshida, K. Matsumoto, and T. Hashimoto, "High Efficient two-Stage gm Refrigerator with Magnetic Material in the Liquid Helium Temperature Region," in *Advances in Cryogenic Engineering: Part A {&} B*, R. W. Fast, Ed. Boston, MA: Springer US, 1990, pp. 1261–1269.

[4] T. Hashimoto, M. Ogawa, A. Hayashi, M. Makino, R. Li, and K. Aoki, "Recent progress on rare earth magnetic regenerator materials," in *Advances in Cryogenic Engineering*, Springer, 1991, pp. 859–865.

[5] S. Fujimoto, K. Kazami, Y. Takada, T. Yoshida, H. Ogata, and H. Kado, "Cooling of SQUIDs using a Gifford-McMahon cryocooler containing magnetic regenerative material to measure biomagnetism," *Cryogenics (Guildf).*, vol. 35, no. 2, pp. 143–148, 1995.

[6] M. J. Eshraghi, I. Sasada, J. M. Kim, and Y. H. Lee, "Characterization of a low frequency magnetic noise from a two-stage pulse tube cryocooler," *Cryogenics (Guildf).*, vol. 49, no. 7, pp. 334–339, 2009.

[7] T. Morie, T. Shiraishi, and M. Xu, "Experimental investigation of cooling capacity of 4K GM cryocoolers in magnetic fields," *Phys. Procedia*, vol. 67, no. 2003, pp. 474–478, 2015.

[8] E. L. Hershberg, I. E. Anderson, M. G. Osborne, M. F. Hundley, and J. L. Smith, "Advances in Cryogenic Engineering Materials : Volume 40, Part A," R. P. Reed, F. R. Fickett, L. T. Summers, and M. Stieg, Eds. Boston, MA: Springer US, 1994, pp. 617–624.

[9] N. V Tristan, K. Nenkov, K. Skokov, and T. Palewski, "Specific heat and magnetic susceptibility of intermetallic compounds R 3 Ni," vol. 344, no. 0921, pp. 462–469, 2004.

[10] L. Temperatures, "Magnetization of Er3Ni single crystals," vol. 158, pp. 405–406, 1996.

[11] C. Bécle, R. Lemaire, and D. Paccard, "Experimental Evidence for Anisotropic Interactions in

Some RareEarth Intermetallic Compounds The Mott Transition-Anisotropic Exchange," vol. 855, 1970.

[12] E. Talik, "Magnetic and transport properties of the R , Ni system (R = Y , Gd , Tb , Dy , Ho , Er)," vol. 193, pp. 213–220, 1994.

[13] K. H. J. Buschow, "Intermetallic compounds of rare-earth and 3d transition metals," *Reports Prog. Phys.*, vol. 40, no. 10, p. 1179, 1977.

[14] M. Ogawa, R. Li, and T. Hashimoto, "Thermal conductivities of magnetic intermetallic compounds for cryogenic regenerator," vol. 31, pp. 405–410, 1991.

[15] Y. Tokai, A. Takahashi, M. Sahashi, T. Hashimoto, H. Yayama, and A. Tomokiyo, "Magnetic Field Influence on Er 3 Ni Specific Heat," *Jpn. J. Appl. Phys.*, vol. 31, no. 10R, p. 3332, 1992.

[16] K. Rajendra, "Finite Element Analysis of Magnetic Field Effect on Refrigeration System,", Master's Thesis, LPU, 2016.

[17] S. Jeong and J. Smith Jr., "Magnetically Augmented Regeneration in Stirling Cryocooler," in *Advances in Cryogenic Engineering SE - 172*, vol. 39, P. Kittel, Ed. Springer US, 1994, pp. 1399–1405.

[18] H. Yayama. and Y. H. and Y. M. and A. Tomokiyo, "Hybrid Cryogenic Refrigerator: Combination of Brayton Magnetic-Cooling and Gifford-McMahon Gas-Cooling System," *Jpn. J. Appl. Phys.*, vol. 39, no. 7R, p. 4220, 2000.